Biophysical Chemistry 5 (1976) 55–75

A TELEVISION SCANNER FOR THE ULTRACENTRIFUGE. II. MULTIPLE CELL OPERATION

Darrel L. ROCKHOLT, Christopher R. ROYCE* and E. Glen RICHARDS**
Pre-Clinical Science Unit, V.A. Hospital and Department of Biochemistry, The University of Texas Health Science Center, Dallas, Texas, USA

The "Optical Multichannel Analyzer" (OMA) is a commercially available instrument that with the absorption optical system of the ultracentrifuge, provides an entire 500 channel intensity profile of a cell in real time. With its own analog-to-digital converter, the OMA integrates a selectable number of 32.8 msec scans to provide a time-averaged image in digital form. This paper describes an interface-controller for operation of the OMA with single- and double-sector cells in multicell rotors, simulating double-beam measurement required for absorbance determinations. The desired sector is selected by "gating" the intensifier stage of a "Silicon Intensified Target" vidicon (SIT) used as the light detector. The cell location in the rotor and the position of the gate relative to the cell centerline is obtained from a phase-locked loop circuit which divides each rotation of the rotor into 3600 parts independent of rotor speed. (This circuit employed with photomultiplier scanners would select the gate position for integration of photomultiplier pulses.) From examination of appropriate signals with an oscilloscope, it was verified that gate positions and widths are located with an accuracy of 0.1° or better and with a precision of ±0.1 μs. The light intensity profile for any desired cell can be examined in "real time", even during acceleration of the rotor. Additional circuits employing a 10 MHz crystal clock 1) control the automatic collection of data for all sectors in multicell rotors at digitally selected time intervals, 2) display the rotor speed, and 3) indicate the elapsed time of the experiment. Constructed but not tested are additional circuits for pulsing a laser into the absorption or Rayleigh optical system. The accuracy of the pulsed SIT has been demonstrated by measurement of absorbances of solutions and also by sedimentation equilibrium experiments with myoglobin. The estimated error is 0.003 for absorbances ranging from 0 to 1. The interface-controller operates extremely well, but problems related to the pulsed SIT (optimum gate position relative to the sector opening shape of high-voltage pulse, slight pincushion distortion) require more work.

1. Introduction

Among the various methods used for recording concentration distribution information from the ultracentrifuge, the absorption optical system enjoys the honor of being a part of the inception and construction of the first ultracentrifuges [1]. However, the difficulties encountered in the recording of the light intensity on photographic emulsions and the subsequent photometry of the images led workers in the next decade to abandon absorption measurements in favor of more accurate and easily performed refractometric methods.

* Present address: 45 Rose Ave., No. 18, Venice, California 90291, USA.
** Please address all correspondence concerning this paper to: E. Glen Richards, VA Hospital, 4500 S. Lancaster Road Dallas, Texas 75216, USA.

Requirements for measurements on nucleic acids at the lowest possible concentration led to the revival of absorption optics in spite of the difficulties. Early in the 1960's, developments in electronic components and circuitry led to the development of "photoelectric scanners" in which the radial distribution of light intensity was obtained with a single photomultiplier tube behind a slit, either by moving the photomultiplier along the image [2,3] or by deflecting the image to the stationary assembly with an oscillating mirror [4]. With these instruments it became possible to obtain recorder traces within a fraction of a minute, depending upon the rate of movement of the component being scanned. However, considerable time and subjective decisions were required in converting the traces into absorbance and radius information needed for quantitative evaluation of the experiment being performed. The addition of minicomputers to photomul-

tiplier scanners led to "on-line" processing of the data, with some improvement in accuracy. Papers presented at this conference represent most recent advances in improvements to these systems. However, there are a number of disadvantages to the use of a photomultiplier as a light detector, the main ones being (1) the necessity of throwing away all of the light at the image that is not at the slit and (2) radial warpage of absorbance data from precession of the rotor.

With further improvement in electronic components and circuitry and the recent development of stable, relatively inexpensive television camera tubes, it became possible to develop light detectors for the absorption optical systems that would examine the entire image without wasting any of the light. The first published use of a vidicon television camera was by Lloyd and Esnouf [5], who described a split-beam system with solvent and solution images presented side by side on the vidicon face. During the scanning by the electron beam at each radial position, digital and analog circuits give the absorbance difference, with the entire absorbance profile being presented to an oscilloscope or to a recorder. In independent work we described the use as a scanner of a commercial instrument, the "Optical Multichannel Analyzer" (OMA) with a television camera tube [6]. Even though results from absorbance and sedimentation equilibrium experiments demonstrated the accuracy of the system, the OMA had the ability to examine only a single-sector cell together with a counterbalance cell in a two-hole rotor.

In this paper we will describe an OMA-ultracentrifuge interface controlier that permits the examination of images and the recording of data from single- and/or double-sector cells in two-, four-, or six-hole rotors. The desired sector in the rotor to be viewed is selected by "gating" the intensifier state of a "Silicon Intensified Target" (SIT) vidicon. The cell location relative to a mark on the rotor and the signal for opening and closing of the gate is obtained from a phase-locked loop circuit which divides each rotation of the rotor into 3600 parts, permitting the location of angular positions to better than 0.1°. (This circuit employed with photomultiplier scanners would also locate cell positions in the rotor and select angular gates for the integration of photomultiplier pulses.) Any desired cell can be examined in "real time", even during acceleration of the rotor. Additional circuits provide for the continuous measurement of rotor speed and for automatic collection of data at preselected times. Not described in this paper is additional circuitry which permits the use of a pulsed laser with the absorption or Rayleigh optical systems.

2. Equipment

A short, vertical optical tube containing a movable camera lens was fastened to the upper plate of the Beckman Model E ultracentrifuge in line with the vertical axis of the chamber lenses of the conventional absorption optical system as already described [6]. An H85C3 mercury arc lamp was used as the light source. A small micrometer stage, Nikon Type B, was fastened to the top of the tube. The OMA Model 1205A console and Model 1205D SIT detector assembly (Princeton Applied Research Corporation, Princeton, NJ) was used as the light detector and scanner. Coupled to the OMA were a Model 604 display monitor with a $6\frac{1}{2}$ in. cathode ray tube (Tektronix, Inc., Beaverton, OR), an Omnigraphic 2000 $X-Y$ recorder (Houston Instrument, Houston, TX), and a 700 ASR Electronic Data Terminal with cassette tapes (Texas Instruments, Inc., Dallas, TX). An interface card in the OMA console permitted recording and printing data at 30 characters/s or recording only at 120 characters/s.

During construction and evaluation of the interface-controller a Model 465 100 MHz oscilloscope (Tektronix) was used to examine and evaluate electronic signals.

The optical system was aligned as described earlier [6], except for several modifications. After correct positioning of the light source the light beam from the condensing lens was interrupted by a ground glass held about 35 cm above the upper plate by a clamp on a small ringstand. The location of the beam was marked. The optical tube with camera lens was placed on the plate and tightened in the position where the light beam remained centered at the mark. The micrometer stage with adapters and then the SIT detector assembly were fastened in place.

The horizontal positioning of the detector assembly is rapidly performed. The head is moved front-back to center the pattern on the monitor, then left-right until part of the pattern moves below the horizontal zero lines, indicating that the image has crossed into the

correction portion of the vidicon scan pattern [6]. Rotational adjustments with the goniometer on the stage are made until the pattern is observed to decrease and pass evenly through the zero line as the stage is moved left-right.

3. Description of OMA

To facilitate the discussion to follow, the commercial OMA with its detector unit will first be described. The image to be examined is focused onto the active surface of the vidicon camera tube in the detector head. The target area scanned by the vidicon is rectangular in shape, 12.5 mm long by either 5 or 10 mm wide, depending upon the vidicon. The longer dimension, divided into 500 channels, is scanned repetitively each 32.8 ms. The light flux striking the photosensitive face of the vidicon produces a decrease in charge that is integrated until the scanning electron beam "reads" the amount of charge and restores that part of the face to the original state. The target area is divided into two equal rectangles; the division line being in the radial direction. The image is presented to one rectangle while the other is used for a partial dark current correction. The amplified signal from the detector head is passed to the console, where it is integrated and converted to a digital number. As the electron beam scans a given channel in the image rectangle, immediate dark current correction for that channel occurs as the beam continues its passage into the dark rectangle. To obtain a time-averaged image, the counts for each channel are accumulated into separate storage registers for a selectable number of scans from 1 to 9999. Two separate 500-word memories are available for storage of two accumulated images. The registers can store up to 99,999 counts each, but they can be allowed to overflow any desired number of times, permitting a greater signal accumulation to further reduce the error of background noise.

A built-in digital-to-analog converter generates a signal appropriate for driving a cathode ray tube monitor. Either the real-time image, either of the stored images or their difference can be viewed in this manner. A slower analog output is available for plotting the stored images.

The digital intensity information in the OMA memories can be transmitted to a variety of terminals, printers, tape drivers, or computers at selectable rates. Signal inputs and outputs are available for remote operation of many of the OMA functions.

4. The OMA as a scanner for the ultracentrifuge

In a previous publication [6] we explored the feasibility of the OMA as a scanner for the ultracentrifuge. The flashes of light produced by the spinning rotor are not directly observable on the monitor. The light flashes are stored on the vidicon target until read by the scanning electron beam every 32.8 ms. The effect of the sinusoidal variation in light intensity from the 60 cycle ac mercury lamp is to produce a pulse of small amplitude, about 2% of the total signal, that travels across the screen. The effect of the spinning rotor is more complicated. At constant speed the integrated light stored on the vidicon during each scan period is obtained from a number of light pulses which is either of two adjacent integers. The appearance on the monitor is that of either a series of positive pulses traveling toward lower channel numbers (smaller radius) or a series of negative pulses traveling in the opposite direction. The magnitude of the pulses decreases with increasing speed. For example, at 20000 rpm the 10 or 11 pulses per scan produce negative pulses.

A theoretical analysis revealed that after the accumulation of several hundred scans, the effect of rotor and light-source pulsing became negligible. In fact, successive images obtained from a cell filled with solvent were reproducible, with an average difference throughout the solution region equivalent to less than 0.003 absorbance units.

It was mentioned earlier that a channel-by-channel dark current correction is made between the image on one side of the vidicon and the dark region below it. However, the photon-to-electron conversion properties are not identical over the light sensitive surface of the vidicon. Thus, the dark current correction is used mainly to ease the requirements for the analog-to-digital convertor. For an accurate dark current correction it was necessary to block the light passing through the system and accumulated a "dark" image for the same number of scans. With the image in one memory and the dark correction in the other, the difference representing the light intensity was printed or plotted

channel by channel. The overall appearance of the subtracted pattern is much like light intensity patterns obtained from the photomultiplier scanner.

In experiments with dye solutions, one cell at a time in a spinning rotor, it was demonstrated that absorbance values from 0 to 1 were measured with an accuracy of 0.003 units, independent of the speed. Further verification of the accuracy of the OMA came from sedimentation equilibrium studies on myoglobin samples. Plots of the logarithm of the absorbance versus the radius squared were linear. The average difference in absorbance between the experimental points and the calculated straight line was about 0.003 absorbance units, and the calculated molecular weights were in satisfactory agreement with the known values.

In conclusion, our previous work demonstrated that, even in single-beam operation, the OMA as a scanner for the ultracentrifuge performed as well or better than photomultiplier systems in double-beam operation. However, although the vidicon as a light sensor outperforms the photomultiplier in its ability to examine the entire cell simultaneously, it cannot easily be made to select individual cells in a multicell rotor. A number of photomultiplier systems that will examine two or more cells are already available. Therefore, before the OMA system could be considered seriously as a scanner, a method of multicell operation needed to be developed.

5. OMA and multiple-cell operation

We have previously considered three methods of achieving multiple-cell operation with the OMA: a split beam optical system, a pulsed light source, or a gated image intensifier tube between the optical system and the vidicon tube. Re-evaluation of the three methods is warranted because of recent developments.

We had already examined a split-beam system with a half-wedged window to separate the light beams from a double-sector cell and a cylinder lens to focus an image of the two cells on the vidicon face [6]. The side-by-side images as examined photographically were of sufficient quality to warrant further refinement. Moreover, the manufacturers of the OMA now have available circuitry that permits use of the two halves of the detector as separate 500 channel detectors, with simultaneous accumulation of both images.

Lloyd and Esnouf [5] have described a split-beam system with a vidicon scanner that employs a pair of indepedently adjustable mirrors to direct the beams from the normal and wedged cells to the two halves of the vidicon tube. Their logic and analog measuring circuits are entirely different from those used in the OMA. During each line of the video scan, the output signal from the vidicon is separated for the sample and solvent cell. The signals from the two cells pass through a logarithmic amplifier and are then subtracted to give a final signal whose amplitude is directly proportional to the absorbance of the solution. However, the accuracy of the absorbance measurements depends upon both the uniformity of response of the light-sensitive vidicon surface and the linearity of the logarithmic amplifier.

Since the vidicon tubes available with the OMA definitely do not have uniform surfaces, this approach could not be used to obtain direct absorbance measurements for each line of the video scan. A dark current correction is required for each cell scanned.

There is another disadvantage associated with split-beam systems. Whatever optical means that we could visualize for diverting the beams arising from differently wedged cells, the beams passed through different regions of the condensing and camera lenses. Hence, no matter how much care would be taken in the cleaning of the lenses, there would always remain the possibility that the deposition of oil or dirt on one of the lenses could lead to errors in absorption measurement for at least part of the cell. We decided that it would be more profitable to explore and refine single-beam methods, since they could be subsequently adapted for split-beam operation if the above objections appeared not to be serious.

In deciding which of the other two approaches to use for multicell operation, pulsing a light source or an image intensifier, we had to consider the cost and availability of the added components. An important consideration was our requirement for the study of proteins at concentrations in the microgram per milliliter range. Such experiments are most easily performed by illuminating the cell with light in the 220–230 nm range where proteins have very high extinction coefficients [7]. The mercury–xenon lamp and the Beckman DU monochrometer generally used with photomultiplier scanners provide only limited light in this wavelength region. Even though xenon lamps can

be pulsed for the necessary short intervals, the lamps used for pulsing do not have a small, intense arc necessary for illuminating the small slit of a monochrometer. The addition of mercury to xenon lamps enhances the uv spectrum, but the lifetime of excited mercury atoms in the lamp is too long to permit short pulses of the necessary several microseconds' duration. There are several tunable pulsed dye lasers available commercially that would be suitable for wavelengths in the visible region; their cost is high but not exorbitant. The addition of a frequency doubler to such units might provide sufficient light in the 260–280 nm region, but not in the required 220–230 region. However, it is our belief that a pulsed argon laser with a frequency doubler designed for the laser would provide sufficient light in the 260 nm region to be suitable for the study of nucleic acids.

The third approach for multicell operation, pulsing an image intensifier, offered a number of advantages, with only several disadvantages that were not serious. The manufacturer of the OMA had already constructed a detector head assembly with a SIT vidicon tube, which is a commercial unit with an intensifier stage coupled directly to a silicon vidicon tube. Moreover, they had already demonstrated that their particular tube model could be successfully gated, even though it had not been designed by the tube manufacturer for this mode of operation.

Since this approach is the one that we selected, a brief description of the SIT tube will prove useful for the discussion to follow. The fiber-optics face plate of the SIT transfers the image to the photocathode surface with but little loss of resolution. The photons striking the photocathode surface (curved to reduce electron-imaging distortion) release electrons, which are imaged by an electrostatic focusing coil onto the silicon target of the vidicon section. The signal from the scanning electron beam of the vidicon is directly proportional to the light intensity striking the corresponding region of the intensifier face plate. With appropriate accelerating voltages applied to the photoelectrons, a target gain ranging from 1 to about 1800 times can be realized. Thus the SIT can be adjusted to handle a wide range of signal intensities. Even though the "noise" from the SIT increases with gain, at very low intensities with maximum gain the SIT offers reduced signal-to-noise ratio as compared to the standard silicon vidicon. At minimum gain the noise of the SIT is comparable to that of the silicon vidicon.

In steady-state operation of the SIT the focusing coil is more positive than the photocathode. For operation of the SIT in the gated mode the focusing coil is made more negative than the photocathode, thereby turning off the intensifier stage. It can be turned on during the application of flat-topped, positive pulses of the right amplitude, thereby restoring the correct focusing condition. The operating characteristics of the intensifier stage are such that a change of photocathode voltage requires careful adjustment of the pulsed voltage to obtain the sharpest image. Conversion from the steady-state to the pulsed mode is accomplished with a switch in the detector head.

There is an unavoidable problem encountered in pulsing the SIT that was discovered earlier by the manufacturers of the OMA. In normal operation of the vidicon, the target is scanned continuously by the electron beam. However, in the pulsed mode the sharp rise and fall of the high voltage pulse generates interference that is picked up by the preamplifier and video processor circuits located within the same housing as the SIT. Thus it is necessary to pulse the SIT only when the vidicon is not scanning. The OMA already has a delay control to allow accumulation of a weak image on the vidicon face for a desired number of cycles. For pulsing the SIT the number of delay cycles is selected from the OMA console. A logic signal from the appropriate place in the OMA circuit tells when scanning is in progress. This signal can be used to stop pulsing of the SIT during the scanning cycle.

Before the design and construction of a pulsed system for the OMA in operation with the ultracentrifuge, we performed preliminary tests with the SIT operated in the continuous mode. Sedimentation equilibrium experiments with sperm whale myoglobin were performed as described elsewhere [6] for the uv silicon vidicon. With the SIT operated at maximum gain, scatter in the points obtained for the plots of ln absorbance versus radius-squared was only slightly greater than that obtained for the silicon vidicon.

To test the SIT in the pulsed mode, a prototype power supply designed specifically for this purpose was obtained from the manufacturer of the OMA. This power supply provided a variable voltage with adjustable pulse widths and delays. A reference pulse from the counterbalance in the spinning rotor was ob-

tained from the Schlieren–Rayleigh optical system. A DC tungsten filament lamp was placed over the AH-6 lamp housing, and a photodetector was attached to the plate holder at the region corresponding to the inner hole. With the cylinder lens removed to increase the light intensity, there was sufficient signal from the photocell and additional circuitry to provide a reference pulse. A phase-locked loop circuit located the cell positions for a four-cell rotor. At medium and low speeds it was possible to adjust the delay and width of the high voltage pulse such that an image of any desired cell in a four-cell rotor could be viewed. The optimum image for any cell was obtained when the pulse width was about the same size as the sector opening of the cell. After several days of testing and the measurement of image intensities, we were convinced that the image quality was equal to that obtained from the SIT operated in the continuous mode.

6. Description of the interface-controller

6.1. Preliminary design considerations

Once we were satisfied that the SIT could be successfully gated, we had to decide how much of a system to build for a thorough and accurate evaluation of results from quantitative absorption experiments. Rather than going through the time-consuming process of constructing a series of progressively improved prototypes and repeating the same tests, we decided on one well-built prototype with resolution capabilities finer than needed.

An important design consideration was that the system ha.' to be able to handle both single- and double-sector cells. With the latter it would be possible to use a number of cells in the same rotor, each with a different solvent. We were uncertain as to the ability of the pulsed SIT to be gated so as to avoid accumulation of light from the adjacent sector. It was almost certain, however, that the gating of single-sector cells would be successful. For this case it would be necessary to use separate cells for the solution and solvent profiles required for absorbance measurements.

Before a pulse-width selection system could be designed, the gating requirements for the ultracentrifuge had to be evaluated. Since the SIT integrates the light flux received during the gated time period, the output signal is proportional to the gate width. The maximum signal occurs when the gate and the cell widths are the same. Thus it would seem that the ideal gate would be somewhat wider than the cell to allow for blurring due to the lateral extension (perpendicular to the radius) of the light source and the aperture slit above the rotor. However, even slight variations in the sector openings for solution and solvent cells (or sectors of a double-sector cell) would lead to errors in absorbance calculations. Such errors could presumably be corrected, channel by channel, from a separate experiment with solvent in both cells to determine any variation in cell widths. This problem with nonidentical sectors could be eliminated by gating sufficiently inside the sector to avoid the blurred region. However, our pulsed power supply requires about 1 μs each rise and fall time. During these periods of reduced voltage the electron image in the intensifier stage suffers varying degrees of defocusing, so that an unknown part of the output signal is reproducible but unwanted noise. Presumably the output pattern could be corrected by subtracting an image of the same cell obtained with a narrow pulse width. This defocusing effect is not important if it occurs in a "dark" region, as would be the case for gating just outside of the cell opening. Thus a thorough evaluation of both approaches required an accurate and reproducible selection of gate widths with as small an increment as possible.

It was necessary to find a suitable method of generating the delays and pulse widths necessary for selecting various cell positions for multicell rotors and variable gate widths for single- and double-sector cells that would be reproducible, independent of speed, and suitable for automatic operation. Even though circuits with resistors and capacitors could be easily constructed that would permit tuning the pulse width and its delay for viewing any desired angle of a spinning rotor, such tuning would be neither reproducible nor independent of rotor speed. A digital time-delay generator with a quartz crystal clock [8] would satisfy the reproducibility requirement, but it would not be independent of rotor speed.

We considered two methods that would be independent of speed: (1) counting crystal clock pulses during selected rotor revolutions and performing digital arithmetic to calculate cell positions and gate widths, and (2) using a phase-locked loop circuit to generate precise angular divisions during each rotor

revolution that could be counted to find the cell positions and to select the gate widths. We selected the second method because of simpler circuitry. We did not consider the use of a minicomputer for this purpose, although it is now evident that such an approach is well suited to a MaD French-speaking system [9].

As discussed in our earlier paper on the OMA [6], variations in lamp intensity and gain in the preamplifier stage of the SIT lead to variations in the amplitude of the integrated patterns. We found that a correction of intensities based upon the relative heights of one of the reference holes eliminated the effect of these variations. A similar correction for the pulsed SIT required that it be pulsed for both the reference cell and the selected cell for every revolution of the rotor.

In our previous work the dark-current correction was obtained with a shutter blocking the light to the vidicon. Rather than using a mechanical shutter for this purpose, we decided to pulse the SIT at times when an opaque region of the rotor passes through the light beam. This approach is better in that stray light entering any part of the optical system above the rotor would be subtracted from the final image.

To handle the time delays involved in the digital circuitry and the pulsed power supply for the SIT, we decided to incorporate digital timing based on a quartz crystal clock. Using the photography exposure and interval timing mechanism already in the ultracentrifuge to control automatic data gathering would have saved time and money. For greater accuracy, convenience and flexibility in the operation of the controller, we included a digital timing system based on the crystal clock for this purpose. With the angular measurement of the rotor and the digital time both available, it was relatively simple to include the continuous measurement and display of rotor speed. Since we also had need for a pulsed laser with Rayleigh interference optics, we included a control system for pulsing a laser into either optical system.

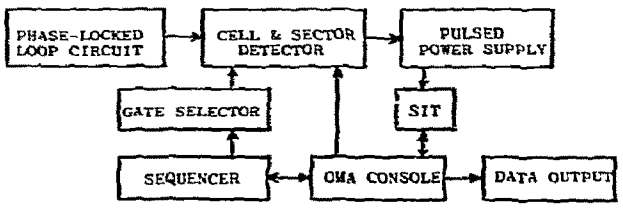

Fig. 1. Systems block diagram of the interface controller.

6.2. Systems block diagram

Fig. 1 shows the systems block diagram of the final interface-controller unit. A mark detector circuit locates the approximate zero-degree position of the rotor, as obtained from a mark on the rotor corresponding to the center of the counterbalance hole. A phase-locked loop circuit divides each rotor revolution into 3600 parts, thereby generating "Angleclock" pulses corresponding to 0.1° intervals. These pulses are counted to detect cell positions and also selectable gates for pulsing the SIT in phase with the spinning rotor. Controls are included for automatic or idle (real-time) selection of the cell to be viewed. Exposure controls permit the timing of the sequencer, which selects the cells to be viewed during automatic data accumulation. The sequencer also operates the pulsing of the SIT and the automatic data accumulation in the OMA console, from which the accumulated data are transferred to a storage device. Additional circuits (not shown) for pulsing a laser into either optical system will be described elsewhere. Important aspects of the circuits will be described in greater detail.

6.3. Location of reference mark on rotor

To accurately locate cell positions around the spinning rotor, there must be provided a reference pulse corresponding to a precise physical position on the rotor. Since the controller was being designed for use with both optical systems, the permanent alteration of either system to provide a reference pulse would not have been convenient.

Our initial design concept was to measure angular locations with an accuracy of 0.1°. Being unsure of the performance of the as yet undesigned electronic circuitry, we wished the location of the reference mark to be much better than 0.1°, say 0.05° or less. The manufacturer of the commercial photoelectric scanner for the Model E ultracentrifuge provides a multiplexer system for multicell operation which utilizes a marked coding ring and a modified rotor support fork with a pair of lights and photodetectors. The dual sensor and specially marked coding rings provide not only a reference position for the rotor but

also pulses for locating cell positions for various multicell rotors. Since the outer radius of the rotor in the region of the cells is about 9 cm, six times that of the coding ring with its 1.5 cm radius, it is clear that for a given rotational speed and the same light-to-dark transition of a coding mark, the pulse rise time would be about six times faster at the larger radius. Thus we decided to mark the outside of the rotor and to construct our own light source and detector system.

The black, anodized surface was removed from a small, rectangular region on the side of a four-hole AN-F rotor, leaving a relatively shiny stripe about 9.5 mm high by 2.0 mm wide, with the leading edge placed as close as possible to a radius through the center of a rotor hole number four. As measured with a seven-power eyepiece, the roughness of the edge is 0.1 mm, equivalent to a maximum 0.06° uncertainty in its location. A bracket attached to the rear of the rotor support fork behind the condensing lens holder supported the light source and photodetector mounted in a vertical line. For the light detector we selected the Monsanto silicon PIN photodiode MD2. This detector has a very fast rise time of 0.5 ns and a domed lens to improve the optical gain. Because of the limited space between the edge of the rotor and the inside surface of the chamber, a small light source was required. An attempt to use a compact light-emitting diode as the source was unsuccessful due to dispersion of the light beam after reflection from the cylindrical rotor surface and to insufficient contrast between the shiny black surface of the rotor and the somewhat rough surface of the stripe. Sufficient light was obtained with a 6 V, 0.15 A flashlight bulb operated at 5 V and a planar mirror and lens to focus the filament onto the stripe. The wires for the lamp and detector were passed through our version of the vacuum-sealed, feed-through plate at the top of the chamber. To reduce spurious signals easily picked up by the wire with the low-level signal from the photodiode, a circuit with an amplifier, comparator, and a 74S140 dual line driver were placed in a closed box next to the rotor drive unit. This circuit provided a pulse with a sharp rise time corresponding to some point on the slowly rising portion of the pulse from the leading edge of the stripe. It was later found that the switching on of electrical components like the plate-drive motor and the solenoid-operated photographic shutters produced noise pulses in the mark-detector circuit that interfered with the phase-locked loop circuit. Reducing the amplitude of the noise by the addition of appropriate resistors and capacitors to the circuits of each of the offending components eliminated the interference problem.

6.4. Phase-locked loop

The phase-locked loop is an electronic circuit used for many purposes. In this application it serves as a frequency multiplier which divides the time between successive rotor revolutions, independent of speed, into the desired number of angular divisions. The phase-locked loop integrated circuit consists of two parts, a linear, voltage-controlled oscillator and a phase comparator (fig. 2). The square-wave signal from the rotor-pulse circuit enters the loop circuit and the oscillator generates a signal of greater frequency. This signal is then divided into 0.1° rotor divisions by the "feedback" counter which counts 3600 pulses. (The two stages of this counter will be described later.) If no time delays were involved, the resulting pulse would enter the comparator circuit, which determines whether it arrives earlier or later than the next pulse from the rotor. The frequency of the oscillator is internally adjusted upward or downward in a direction to bring the phase relation between the two signals into closer correspondence. The division, comparison, and frequency adjustment processes are repeated until the two signals are in exact correspondence or "locked". The entire process requires only a few seconds even if the circuit is turned on while the rotor is spinning. The advantage of this approach is that the output signal closely follows momentary changes in rotor speed arising in the speed control circuit. No matter what the speed, if locking occurs, each rotation of the rotor is divided into 3600 equal pulses, which we call "Angleclock".

The pulse from the phase-locked loop circuit cannot be directly used for pulsing of the SIT for three reasons: (1) there is a delay in the high-voltage pulsing circuit for the SIT; (2) the rotor mark may not correspond exactly to the center of the rotor hole; and (3) the sector opening for the cells occurs earlier than the center of the rotor holes. Therefore, to allow for "pretriggering" with respect to both time and angle, two delays are introduced just after the feedback counter. We anticipated that the largest angular

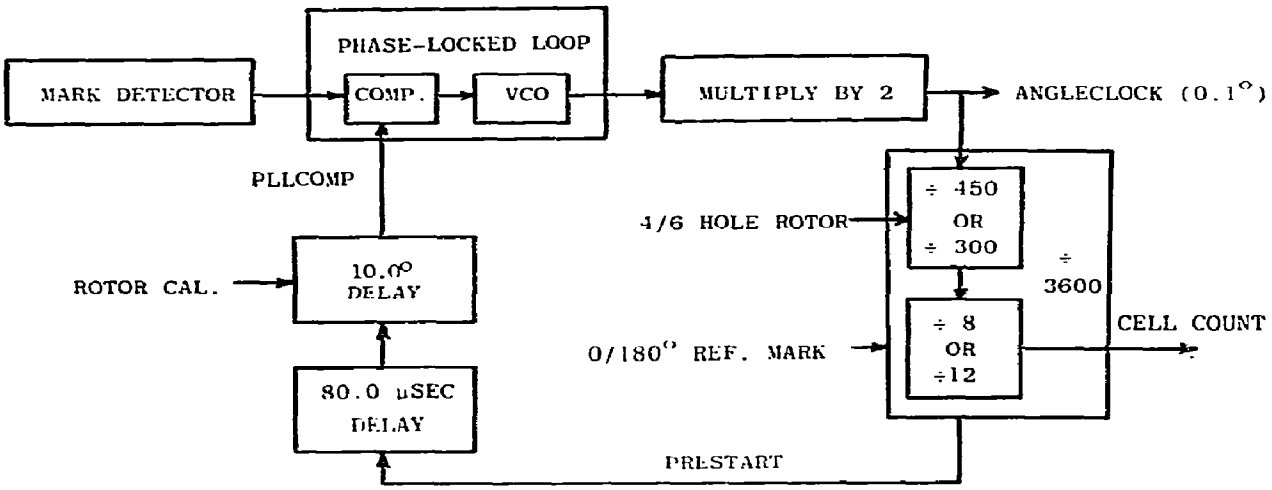

Fig. 2. Flow diagram of phase-locked loop and cell select circuits.

pretrigger would be about 4° from the center of the rotor hole and the largest time pretrigger for a pulsed power supply would be several microseconds. To allow for larger angles and time values, the pulse from the feedback counter was delayed by 800 of the 10 MHz crystal clock pulses (80.0 μs), then by 100 Angleclock pulses (10.0°). Since the pulse after the two delays (PLLCOMP) is the one actually brought into lock with the rotor pulse, the pulse just before the two delays (PRESTART) is used for pretriggering; it occurs 80.0 μs earlier and 10.0° before the rotor mark.

The adjustment for an error in the rotor mark position is accomplished by means of two decade thumbwheel switches that can add or substract Angleclock pulses to or from the 100 Angleclock pulses. The exact pretriggering time could also have been handled as part of the 80 μs counter. Since we anticipated the simultaneous use of both a laser and a pulsed power supply for the SIT, each with a different delay time, pretriggering for each was introduced further in the circuit. Thus the location of the cell centers and sector openings is obtained, in effect, from an analog rotor which travels 10.0° and 80.0 μs ahead of the real rotor.

Phase-locked loop circuits are conveniently obtained as integrated circuits. The range of frequencies over which a given unit will operate is determined by particular values of an external resistor and capacitor. Among the various integrated circuits examined, we originally selected the RCA CD4046AE because it would lock over a wider frequency range with a given resistor-capacitor combination. However, at the maximum voltage of operation (15 V), its maximum frequency output is 1.3 MHz, corresponding to a rotor speed of 22 000 rpm. The effective rotor speed was doubled by introducing a Signetics 8T20 "bidirectional one-shot" integrated circuit between the phase-locked loop integrated circuit and the feedback counter. This integrated circuit in effect, multiplies the pulses from the oscillator by two (fig. 2).

With the best resistor-capacitor combination that we could find, the circuit would lock between 9 000 and 44 000 rpm. Another combination handled speeds from 900 to 9000 rpm. More recently we have used a similar Motorola integrated circuit MC14046AL which operates at up to 18 V to give locking at higher frequencies. With a selected resistor-capacitor combination, it operates from about 17 000 to 39 000 rpm and the addition of the bidirectional one-shot produces locking for twice the speeds, namely 34 000 to 78 000 rpm. Another Motorola integrated circuit used with a different resistor-capacitor produces locking from 500 to 17 000 rpm The desired speed range is selected with a three-position switch. The newer loop components do not lock as fast as the earlier ones, but if the pulsed image disappears during acceleration owing to loss of locking, the image is rapidly restored if acceleration is stopped for several seconds.

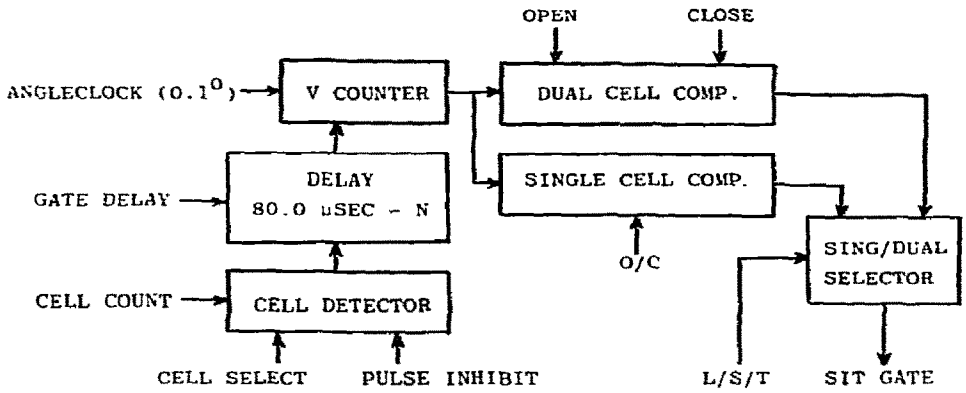

Fig. 3. Flow diagram of cell detector. V counter and gate position and width circuits. L, S and T refer to leading, single and trailing sectors, respectively.

6.5. Cell location

The location of cells for two-, four-, or six-cell rotors is obtained during the division process of the phase-locked loop circuit (fig. 2). Division by 3600 occurs in two stages: first by 450 and then by 8 for the four-hole rotor, or first by 300 and then by 12 for the six-cell rotor. Thus, for the four-hole rotor the successive even numbers of 450 count sequences locate the exact center lines of the successive rotor holes, while the odd numbers locate opaque regions halfway between centers that are used for dark current correction of the SIT. Similarly, for the six-hole rotor the even numbers of 300 count sequences locate the rotor holes and the odd numbers locate the opaque regions. A two-position switch handles the logic necessary for four- or six-cell operation.

The status of the binary-coded second-stage counter, as it counts pulses from the first stage, indicates the location of the various cells and opaque regions. As will be explained later, a comparator between the second counter and cell selection switches determines which of the cells or background regions is to be viewed.

As mentioned earlier the SIT cannot be pulsed during electron-beam scanning of the vidicon stage of the SIT. During this time a signal from the appropriate place in the OMA console (pulse inhibit) blocks passage of cell location pulses to the next circuit (fig. 3).

Also in this region of the circuit (fig. 2) is the necessary logic to handle whether the mark detector is in line with the optical system (0° condition) or is directly opposite it (180° condition). The logic includes another comparator connected to the rotor select switch and a 0/180 switch. For the 0° condition the output pulse representing the completion of the 8 or 12 pulse counting is allowed to proceed directly to the two delay counters of the phase-locked loop. For the 180° condition the pulse corresponding to the second cell from 0° for the four-cell rotor or to the third cell from 0° for the six-cell rotor is sent, instead, to the two delay counters. The introduction of the 180° delay, in effect, transfers the reference mark to the opposite optical system and maintains cell counting relative to the optical system being used.

6.6. Setting of pretrigger times

The pulse leaving the cell selection circuit (fig. 2) indicates the cell center line of the rotor analog and therefore precedes the actual selected cell center line by 80.0 μs and 10.0°. This pulse enters two separate circuits (fig. 3), one handling the SIT gate pulsing and the other handling the laser flashing. As the two circuits are similar and the laser is not used in any of the experiments reported in this work, only the former will be described.

The pretrigger time to the nearest 0.1 μs is set into three decade thembwheel switches. This number is loaded into three BCD up-counters. The pulse from the cell select circuit triggers the counters to start counting 10 MHz crystal clock pulses. These pulses are

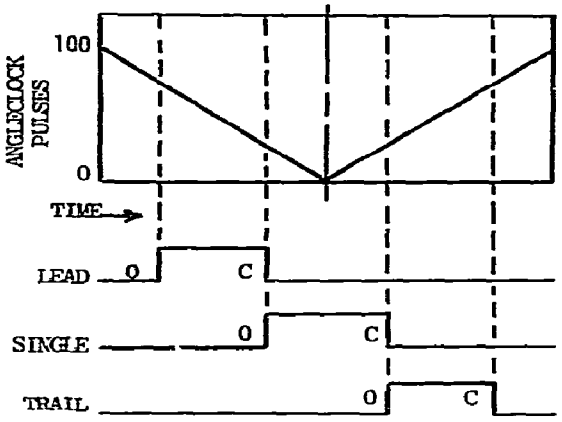

Fig. 4. Schematic representation of selection of gate position and width from V counter.

counted up from the present number to 800. The output pulse has now been delayed 80.0 N μs, where N is the pretrigger time. The original 80.0 μs pretrigger introduced into the phase-locked loop circuit has now been reduced to N, the exact value required for pretriggering the SIT pulsed power supply.

6.7. SIT pulse-width selection for single- and double-sector cells

Pulse widths for the SIT must be correctly positioned for both single- and double-sector cells. The logic to handle both kinds of cells is readily obtained from an up-down counter used in an application which we call a "V" counter. The arrival of the pulse from the gate-delay counter (fig. 3) triggers the V counter to begin counting Angleclock pulses (fig. 4). It counts down from 100 to 0, whereupon it is converted to count upward from 0 to 100. As the V counter passes through 0, the delay generated represents 10.0°, the exact value introduced in the phase-locked loop circuit. Thus the passage of the V-counter through 0 corresponds to the exact cell center line. Because of the pretrigger circuits, the analog location of the cell center line actually precedes the physical rotor by a time corresponding to the required SIT pretrigger.

The Angleclock pulses from the V counter are passed into separate comparator circuits which determine SIT gate positions and widths for single- and double-sector cells irrespective of which is actually being viewed (fig. 3). The status of the V counter is compared in both circuits with the setting on a group of digital switches which select the opening and closing angles for the SIT gate pulse. Since the V counter passes through any number within its range twice, a single switch setting is used to provide an opening and closing angle symmetrically spaced about the cell center line. For a single-sector cell a pair of thumbwheel switches are used to select the desired onehalf angle in increments of 0.1°. This number on the down and up regions of the V counter determines the leading and trailing edge of the pulse used to turn the pulsed power supply on and off. For a double-sector cell, two sets of thumbwheel switches select the opening and closing angle in increments of 0.1° as measured from the cell center. For the conventional double-sector centerpiece with $2\frac{1}{2}°$ sectors separated by a 2° rib, the switches would be set at 3.5 and 1.0. A switch placed in the selector circuit determines whether the leading or trailing sector is to be viewed. In the former case, during the downward part of the V count, the higher number controls the timing of the leading edge of the pulse and the lower number determines the timing of the trailing edge (fig. 4). If the trailing sector is being examined, the lower and then the higher number determines the pulse rise and fall times during the upward phase of the V count.

The comparator outputs of both V counters pass through a 74157 quadruple 2-line-to-1-line data selector. As will be described later, the position of switches determines which of the three pulses pass through the data selector to control the pulsing of the SIT.

6.8. Idle and automatic cell selection

For evaluation of transmission profiles during sedimentation experiments, the ability to manually select the viewing of individual cells is important. During automatic data gathering the sequential viewing of preselected cells is required. The use of a single set of cell-select switches for both functions is undesirable for two reasons. There is always the possibility of having the automatic program begin while the distracted operator is viewing a cell in real-time with the switches set to a new configuration. One or more of the switches could be incorrectly positioned after real-time viewing. To avoid these difficulties separate

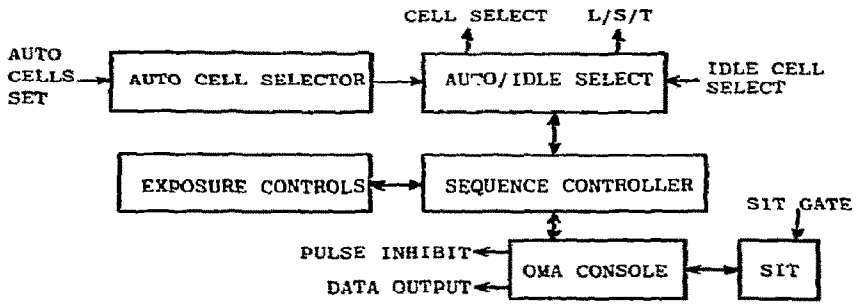

Fig. 5. Flow diagram of automatic and idle cell selector and sequence controller circuits.

switching circuits (fig. 5) were provided for the two modes of operation, "idle" (real-time) and automatic, with the former automatically interrupted or locked out during periods of automatic data gathering.

Selection of the desired cell for viewing in the idle mode is accomplished with a decade thembwheel siwtch with the numbers 0 through 5 corresponding to the cell numbers and the 8 and 9 positions providing the first two opaque regions. Selection between single-sector cells and the leading and trailing sectors of double-sector cells is provided by a three-position switch.

Cell selection for automatic data gathering is accomplished by a horizontal array of three-position toggle switches. The "up" position corresponds to a double-sector cell, while "down" selects a single cell. The center, or "off" position, means that the cell is not to be viewed during automatic operation. During automatic operation the status of each cell switch is transferred sequentially through a 74150 1-of-16 data selector. The output is coded so that the cell numbers for single- and double-sector cells correspond to the coding of the real-time thumbwheel switch. Passage from idle to automatic control of cell selection is accomplished by automatic triggering of another 74157 data selector by the automatic exposure circuit. The output lines of the 74157 (representing binary coded cell numbers) go to the cell detector circuit (fig. 2) for pulsing of the SIT for the correct cell.

Separate three-position switches for real-time and automatic operation control whether a single-sector cell or the leading or trailing sectors of a double-sector cell is to be viewed. Lines for the two control modes also pass through a 74157 data selector to the other 74157 used to select the outputs of the two V counters.

As mentioned earlier, the correction for variation in the light source intensity is accomplished by monitoring the light received through the reference holes in the counterbalance. Thus, during normal operation the circuitry provides for pulsing the SIT for the reference cell and the selected cell during each revolution of the rotor.

If, for some experiments, the omission of the reference holes is desired or a normal cell is placed in cell position 0, a separate switch for idle and automatic operation can be used to eliminate pulsing for the reference holes. The selection between the two modes of operation also passes through a 74157 data selector. The output goes to the cell location circuit which causes the pulsing for both the reference and the desired cell.

Pulsing for the reference cell is controlled by the single-sector V counter even for double-sector cells. This centered pulse provides a better monitor of light intensity. During automatic operation, as will be described later, dark current correction is provided by pulsing the SIT in the first and second opaque regions during each rotor revolution. The two pulses correspond to the reference cell and selected cell. The angular widths are the same as those used for pulsing the cells.

As already described, the pulse inhibit signal from the OMA (fig. 5) enters the cell detector circuit to prevent SIT pulsing during scanning of the vidicon. Since this signal arrives randomly with respect to the light flashes from the reference and solution cells, the circuit logic is constructed to alternate SIT pulsing for the two cells irrespective of when the pulse inhibit signal arrives. In the accumulation of a fixed number of scans for a time-averaged image, there can be at

most a difference of a single light flash for the reference and cell parts of the image. After about 2000 revolutions of the rotor, any error from this source is negligible.

6.9. Automatic exposure controls

To save time and money we could have used the photography exposure and interval timing mechanism already in the ultracentrifuge. For greater accuracy, convenience and flexibility in the operation of the controller we included a digital exposure and interval timing system. Where timing errors would not be accumulative, Signetics 555 timer integrated circuits were utilized; the desired time delay is determined by the value of an external resistor.

An elapsed time clock was constructed from a Mostek 502 50N digital alarm-clock integrated circuit. Provided with a 50 Hz input signal instead of 60 Hz it operates as a 24 hr clock, with the display reading hours, minutes and seconds. When the controller is turned on, the display reads zeroes. It is possible to set the hours and minutes readings to the desired reading with switches. The alarm feature of the circuit can be used to start the automatic data gathering sequences; it can be reset without disturbing the elapsed time.

The exposure and interval timers are set in units of 0.1 and 1 respectively, with three thumbwheel switches. The leftmost switch of each timer goes from 0 to 11, increasing their capacity. A two-position switch selects between the counting being in seconds or minutes.

The exposure number and the elapsed time from the start of each interval are viewed with digital displays. Two digital thumbwheel switches can be set to turn off something or ring a buzzer after a desired number of exposures.

The three groups of switches are also connected to the plate-drive and shutter of the Rayleigh–Schlieren optical system to control automatic photography.

6.10. Automatic data gathering

Control of the OMA for automatic data gathering is handled by the four circuit regions (fig. 5) labelled exposure controls, sequence controller, auto cell selector and auto/real select. A brief description of the events that occur during automatic data gathering will now be given.

It is assumed that various parameters like rotor mark calibration, pretrigger time, four- or six-cell rotor, pulse angle, etc., are correctly selected. The configuration of cells in the rotor is set with the automatic cell selector switches, and the elapsed time clock with the correct initiating time setting is started. At the initiating time the sequence controller, also a 74150 1-of-16 data selector, is entered. If the first cell selector switch indicates a single sector, real-time control is rejected, and the correct cell location is detected. The following operations within the OMA are controlled: (1) the 500 channels in memory A are erased; (2) 3 s (set with a 555 timer) is allowed to elapse to precondition the SIT with light from the selected cell; (3) the selected number of scans on the OMA panel accumulates in the A memory; (4) the B memory is erased; (5) the cell detector circuit selects the first and second opaque regions for pulsing the SIT; (6) another period of 3 s elapses for preconditioning the SIT; (7) the same number of scans is accumulated in the B memory; and (8) the A–B difference of all 500 channels is output to the desired device. Since the two preconditioning times are not digital, the exposure time setting is used to time the beginning of the next data-gathering sequence. When this time has elapsed, the configuration of the second cell-selector switch is examined. If it again indicates a single-sector cell, the entire sequence of operations is repeated, but with the cell detector indicating cell position 2. If any cell-selector switch is in the "off" position, it is rapidly passed over with an insignificant delay in the microsecond range. After all of the cells have been examined in this manner, the toal time since the beginning of the first exposure sequence is allowed to count up to the value set into the interval timer, whereupon the entire set of operations is repeated.

With the cell select switches in the double-sector positions, the leading and trailing sectors are examined sequentially as though they were separate cells. A switch can be positioned to read leading cells or trailing cells only. If the switches are in mixed single- and double-sector positions, each cell position is handled correctly. A switch can also be set to handle the sequential examination of each sector in a triple-sector cell [10], but with no single- and double-sector cells in the rotor.

6.11. Cell select display

For the convenience of the operator in setting up and using the interface controller, a display with a pattern of light-emitting diodes to represent a rotor is provided on the instrument panel. The diodes for a four-cell rotor are placed in the center of the sides of a square which are numbered clockwise, starting from the top, 0, 1, 2, and 3. These diodes represent the counterbalance and three cells passing through the optical system as the rotor spins counterclockwise. Surrounding the square is a larger hexagon oriented with a vertex up. The intersections of the sides, representing the six cells, are numbered clockwise 0–5. In the real rotor the counterbalance is placed in the highest numbered hole (where the rotor mark is also located) which corresponds to position 0 in the terminology for the controller. Thus the correspondence between the numbering of the cells in the real, analog, and "display" four- and six-hole rotors is preserved. Inside of both patterns is the single thumbwheel switch for cell selection in the idle mode.

The same switch which controls the cell logic for four- or six-cell rotors also selects which of the two display patterns is to be illuminated. The cell-select switches for automatic operation cause the illumination of the light for that cell. The patterns also differentiate between a single- and double-sector cell, as determined by the position of the cell-select switches, by the use of one red light or two green lights at each cell position on the pattern. During the ultracentrifuge experiment the sector being viewed is indicated by a flashing of the light corresponding to that cell.

6.12. Rotor speed measurement

The rotor speed is conveniently obtained from the Angleclock signal, whose frequency is 3600 times the speed in revolutions per minute. The number of Angleclock pulses per second is then 60 times the rotor speed. Thus, the Angleclock pulses per second divided by six gives the rotor speed directly in units of tenths of a revolution. The speed, measured for a second every two seconds, is continuously displayed.

6.13. Digital time bases

A number of time bases are required for various purposes throughout the circuits. A 10 MHz crystal provides the high speed time base for handling pretriggering times needed for the pulsed power supply for the SIT. Division of this signal by 10 gives a 1 MHz signal for clocking the 74150 1-of-16 data selector integrated circuits. The alarm-clock integrated circuit requires a 50 Hz signal, which is obtained by dividing the 1 MHz signal by 20 000 in one step with a Mostek MK5009P counter time-base integrated circuit appropriately wired. Further divisions of this last signal provide signals with 0.1 s and 0.1 min pulse widths needed for timing intervals for automatic data gathering. Finally, 1 and 2 second pulse widths are obtained for the rotor speed measuring circuit.

6.14. Construction details

Once the necessary performance features had been selected, the usual way of proceeding with a project of this size would have been to design, construct and test each circuit segment. After all of the segments had been made to function satisfactorily, a total design would have been worked out involving the use of optimal components before starting construction. Because of a limited time requirement we decided to build a working prototype with electronic components that were available locally within a few days. The various segments of the interface-controller were designed, constructed and tested in the order of information flow in the circuit.

For a single prototype of this size, the use of commercial wire-wrap boards that accepted standard dual in-line packaged integrated circuit was the best approach. Knowing that a great deal of wiring would be required, we initially purchased an electric wire-wrap gun and a thermal wire stripper. With these tools, the wiring was rapidly accomplished and errors were readily corrected with no damage to adjacent connections. (In retrospect the use of soldering or even a hand-operated wire-wrap tool would have been foolhardy.)

Part way during construction of the circuitry we obtained a box 7 in. high by 17 in. wide by 9 in. deep, believing that everything would fit inside. The positions of the various switches and displays were carefully arranged on the front panel, which was then machined to accept them. By the time construction was completed, there were about 175 integrated cir-

cuit packages. Space was sufficiently cramped that the power supply had to be transferred to another box. If another interface controller were to be built, a bigger box would be used.

Circuit diagrams and additional construction details will be provided upon request.

6.15. Use of the SIT with the OMA

Before the SIT is used in the pulsed mode, certain electronic adjustments are made easier with it operating in the continuous mode. The mode of operation is controlled with a toggle switch in the detector head. To reduce pin-cushion distortion in the intensifier stage of the SIT the line-scan pattern is different from that employed with the simpler vidicon tubes. The line scan is reduced in width and shifted in the same dimension so that image portion of the scan is centered with respect to the faceplate. This adjustment will already have been made if the OMA is supplied with the SIT. The scan voltage can be examined with an oscilloscope and appropriate adjustments are easily made, if necessary.

With the SIT operating in the continuous mode, the optical system is aligned and the camera lens is focused for the wavelength of light being used as described earlier. The pulsed power supply is connected to the SIT which is switched to the pulsed mode. The determination of the correct pulsed voltage is best performed with a single-sector cell filled with water and a counterbalance in a rotor spinning at from about 10 000 to 24 000 rpm. The gate angle is adjusted to about 5° to encompass the entire sector. While looking at the real-time image on the monitor, the pulsed voltage is adjusted to give the sharpest image of the reference edge and the meniscus. The image begins to deteriorate when the voltage is shifted several percent in either direction. At the optimum voltage the pattern looks essentially the same as that obtained in the continuous mode. A change in photocathode voltage requires readjustment of the pulsed voltage.

The target gain provided by the intensifier stage of the SIT is controlled by the accelerating voltage of the photocathode. This voltage can be adjusted with a potentiometer in the detector head. From the value of a low, ac voltage measured at a test point one can estimate the photocathode voltage. An estimated target gain is obtained from a plot relating gain to the photocathode voltage.

Because of increasing noise with increasing photocathode voltage, it is best to operate at the lowest voltage that gives a suitable image in real time at the wavelength of light selected. Large changes in photocathode voltage may result in rotation of the image, requiring a rotational adjustment of the detector head assembly to compensate.

6.16. Determination of pretrigger time and rotor mark calibration

The pretrigger time and rotor mark calibration can only be determined from measurements made at different speeds. Since the time adjustment has smaller divisions than the angle adjustment, the latter is converted to time units. The total pretrigger time = (mark error)/(60 × rpm) + (pulse pretrigger), where the mark error is plus if it leads the center line and minus if it trails. The mark error and pulse pretrigger can be calculated from appropriate measurements at two speeds. More accurate values can be obtained from measurements at several speeds performed in the following manner. The rotor calibration thembwheel switches are set to 0, corresponding to 0 mark error. A rotor with a single-sector cell and a counterbalance is spun at several speeds. The thumbwheel switches for double-sector cells are set at about 3.5 and 0.5. By switching between leading and trailing cells in the real-time mode, one can monitor the light passing through the leading and trailing portions of the single-sector cell, as interrupted by the walls of the centerpiece. The values of the pretrigger thumbwheel switches are adjusted until the leading and trailing patterns are the same. (If the two patterns are tilted in opposite directions, the cell is misaligned.) Greater accuracy can be obtained from accumulated images. The time indicated by the switches is the total pretrigger time required for the equation above. The determination is repeated for several speeds. The mark error and pulse pretrigger are obtained from the slope and intercept of the plot of total time versus 1/rpm.

This measurement must be performed for each rotor. Since our mark-detector assembly is vulnerable to being moved during coupling of the rotor to the driveshaft, we frequently examine the symmetry of the leading and trailing patterns at the beginning of an ultracentrifuge experiment. The rotor calibration switches are adjusted if necessary.

6.17. Operation of interface-controller

In spite of the rather large number of switches on the front panel of the interface-controller, they were arranged in functional groups for ease in selection of the various functions. Once the necessary parameters (pretrigger time, rotor calibration, pulse voltage, and gate angles) are known, the operation of the system for an ultracentrifuge experiment is flexible and relatively simple. Before acceleration of the rotor the switches for 0/180 mark, 4/6 hole rotor, and the mark error for that rotor are set. During acceleration the various cells are examined in real time to determine if the expected is happening. Once the rotor attains the selected operating speed, automatic operation can be begun immediately with the start of the elapsed-time clock or after a present time with the alarm setting. As described earlier, the automatic cell-select switches can be set for any desired configuration of single- and double-sector cells, the exposure timer can be set for the desired time between the examination of successive cells in the rotor, and the interval timer can be set for the desired time between examination of the same cell. Finally, the frame counter can be set to stop automatic data gathering or to alert the operator with a buzzer.

If examination of a cell image in real time reveals that the pattern should be recorded, a switch is used to begin immediately an automatic data-gathering sequence. When the interval time elapses, the next automatic sequence begins, interrupting the manually started sequence if it is still in progress. An immediate accumulation of data from a higher-numbered cell requires that the lower numbered switches be first set to the "off" position. These must be returned to their original configuration before the interval time elapses.

7. Evaluation and discussion

7.1. Performance of interface-controller

Once errors in wiring and logic had been corrected, the interface-controller performed extremely well, in fact, much better than we had expected. We have demonstrated both the durability and ease of installation of our OMA system by dismantling the system (except for the mark detector), shipping the well-packaged components and reinstalling the system on a different ultracentrifuge. The entire operation has been performed twice, first in Dr. Howard K. Schachman's laboratory in Berkeley, Calif. and in Dr. Marc S. Lewis's laboratory in Bethesda, Md. Installation required about two hours. The only difficulty encountered was in the mark-detector system, as we were attempting to adapt modified versions of the Beckman rotor collar to our system. Our experience with these mark detectors will be discussed later. With our ultracentrifuge, we have used only a four-cell rotor with the stripe on the side and our mark-detector system. In the other laboratories we verified that the circuitry controlling pulsing for six-cell rotors performed correctly.

The mark-detector circuit provides a train of pulses with a jitter of ±0.1 μs. Because of the fast rise time of the photodiode detector there is no detectable time difference in the circuit for speeds up to the 52 000 rpm maximum of the AN-F rotor. Except for speeds near the limits of each phase-locked loop circuit, the jitter of the PLLCOMP and Angleclock pulses is about ±0.01°.

The accuracy of the system for location of cell positions has been evaluated by examination of intensity patterns obtained from a rotor with a counterbalance and three single-sector cells spinning at speeds ranging from 10 000 to 52 000 rpm. The pattern for a 4.0° gate width was examined for each cell as the mark calibration was adjusted in 0.1° increments. It was observed that the maximum intensity occurred at the same setting, verifying that not only was the cell location correctly determined by the circuit but the holes in the rotor were drilled in the correct position with an accuracy of 0.1°, equivalent to 0.1 mm at a radius of 6.5 cm.

The gate pulses have been examined many times with the oscilloscope. As determined from the width of the pulses the thumbwheel switches for both the single- and double-sector V counters correctly set the pulse width. When pulse shape was examined at fast sweep rates (equivalent to high magnification) with the oscilloscope triggered from the leading edge of the gate pulse the same total angle set into both V counters produced the identical pulse shape to within the resolving power of the oscilloscope (about 5 ns or better) as the sector selector circuit was switched among the three positions — leading, trailing, and single sector. With the oscilloscope triggered from the

leading edge of the PLLCOMP pulse we have occasionally observed a small, continuous difference between the gate positions for leading and trailing sectors in the double-sector mode. This difference, exactly 0.1 μs or one crystal-clock pulse, arises from a phase difference between Angleclock and crystal-clock pulses. We have never observed the difference when examining gate positions from single-sector cells in a four-hole rotor, but it could occur at speeds that we have not examined. Any error that might arise from a "jitter" in the gate position of one crystal-clock pulse is avoided by making the gate width narrower or wider than the cell opening by several crystal-clock pulses.

Even though time-averaged images are the same for the SIT operated in the continuous and pulsed modes, rotor and light-source pulsing cause different effects on the real-time images. When the SIT is pulsed, the accumulation of light is blocked during target scanning. Rotor and light-source pulsing produce, in this case, time-dependent variations in the real-time image that are the same across the entire pattern, but no travelling pulses as observed for the continuous mode [6]. There are differences in phasing between the reference cell and the other cell positions that are especially noticeable at lower speeds. A simple method for the calculation of accumulated images is not possible owing to the necessity of discarding (1) the fractional part of the number of rotor revolutions during each scan and (2) the revolutions during alternate scans. It would be simple to construct a computer program for handling the calculations. Again, however, any differences between the reference and cell parts of an accumulated image for the pulsed SIT become negligible after several thousand rotor revolutions.

We have verified that the "image" that we use for dark-current correction, obtained by pulsing the SIT for dark regions of the rotor, is the same as that obtained by pulsing the SIT normally but with the mechanical shutter blocking the light path. Even with the optimum light intensity, it is necessary to accumulate about 300 scans for a full-scale time-averaged, image, which requires about 20 sec. The total time required to produce an image with dark-current correction and vidicon preconditioning is about $2 \times 20 + 2 \times 3 = 46$ s. With our cassette terminal requiring about 54 s to receive the digital output from the OMA console, a total time of 100 s is required for each cell image. With other storage devices and approrpiate interfacing, the transfer time could be reduced, the minimum value being 32.8 ms.

7.2. Accuracy of absorbance measurements from pulsed SIT

Our original decision to provide SIT pulse widths in increments of 0.1° was based on the need to determine the gate width that would yield absorbance measurements of the greatest accuracy. Not having a pulsed power supply with negligible rise and fall times, we have been unable to perform the necessary tests. A brief description of problems encountered with narrow pulses having significant rise and fall times is presented later.

To test the accuracy of absorbance measurements from the SIT using moderate pulse widths, we have performed both dilution and sedimentation equilibrium experiments as described in our previous publication [6].

The dilution experiments were performed with a mixture of green and black ink to provide a solution with a relatively flat absorption profile in the visible region, effectively blocking the passage of stray light of other wavelengths. A series of dye solutions, obtained by gravimetric dilution from a stock solution, was sedimented in 4°, single-sector cells in a four-hole rotor; the SIT gate was 3.2°. One of the cells always contained solvent to permit calculation of absorbances. The height of the inner reference hole was used to correct the patterns for variations in light-source intensity. Plots of absorbance versus channel number (fig. 6) are essentially flat. The absorbance values shown outside the plot are those actually obtained at the same wavelength (435 nm) from a Gilford spectrophotometer Model 240 with digital readout multiplied by the cell factor 1.2. The values inside the plot are the mean values with root-mean-square deviations obtained from the OMA. The deviation ranged from 0.003 at low absorbance to 0.02 at the highest value examined. The plot of the Gilford absorbance versus the mean OMA absorbance (fig. 7) is linear with a slope of 1.016 ±0.003. The slight but consistent differences obtained with the two instruments could not have arisen from a difference in effective wavelength, for the absorbance versus wavelength profile of the dye mixture was essentially flat in the 435 nm region.

A further test of the accuracy of the SIT pulsed in-

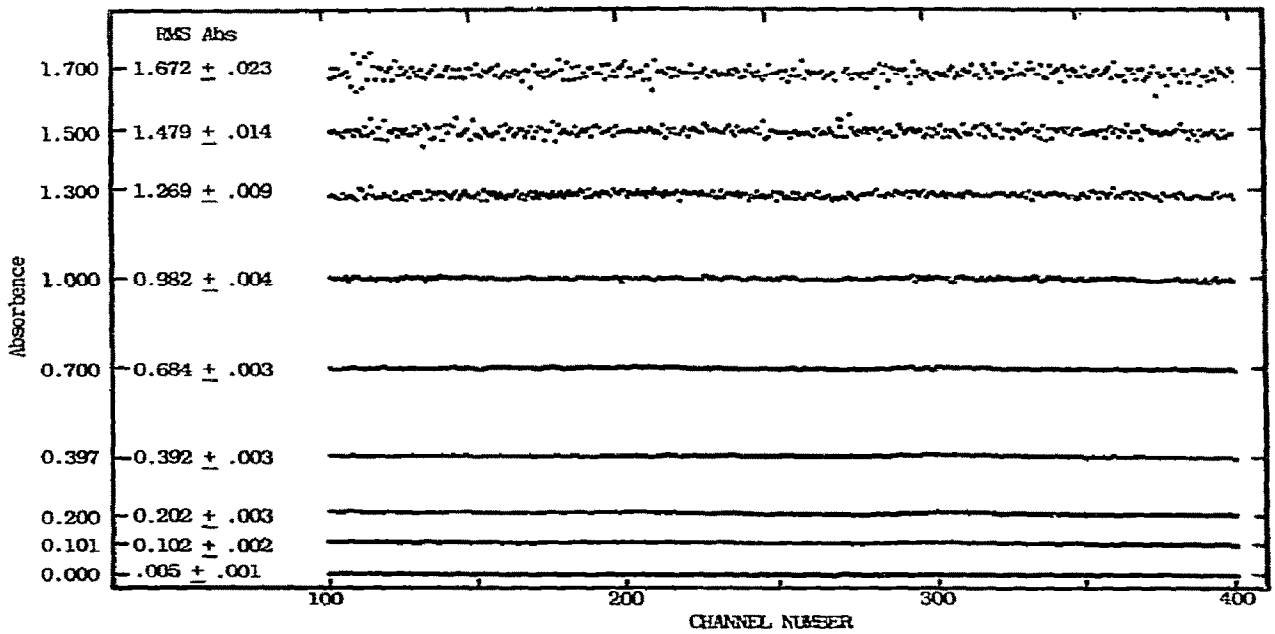

Fig. 6. Radial linearity of absorbance measurements from pulsed SIT. Three solutions at a time were spun at 24 000 rpm in 4° single-sector cells in an AN-F rotor; temperature, 15°; wavelength, 435 nm; 3.2° gate, 360 scans with SIT gain of about 100. The inner and outer reference holes were at channel numbers 28 and 484, respectively.

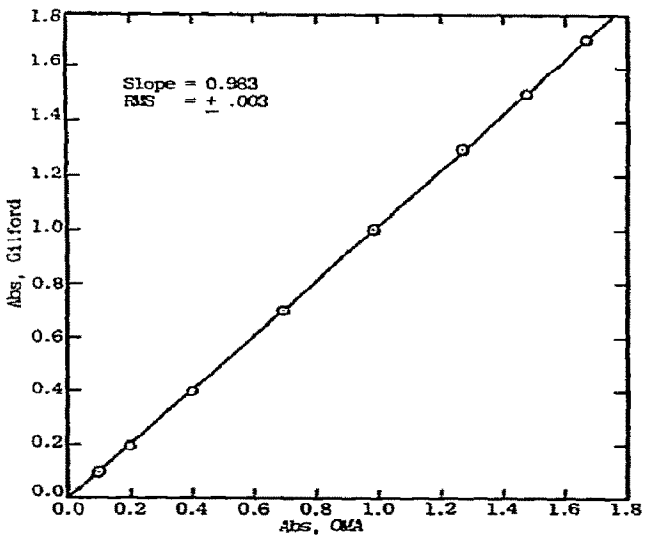

Fig. 7. Linearity of absorbance measurements with the pulsed SIT.

side the cell opening came from a comparison of the absorbance profile with those obtained with the SIT and also the UV vidicon operated in the continuous mode. For the latter two measurements the individual solution (absorbance of 0.7) and solvent cells that had been sedimented simultaneously in the pulsed experiments were sedimented individually. The three absorbance profiles (not shown) had the same average value with deviations of about ±0.003 absorbance units.

Thus the defocusing effect described earlier did not affect the absorption profile, which demonstrates that the warpage alters the intensity patterns for solvent and solution in the same manner.

To further test the accuracy of the SIT with pulse widths smaller than the sector opening, we performed several sedimentation equilibrium experiments on sperm whale myoglobin that had been passed through a G-75 column. The slightly curved plot of the ln absorbance versus r^2 (fig. 8) was straightened by subtracting 0.006 absorbance units from all the values. (We accept the validity of a correction of ±0.006 units on the basis of a possible error equivalent to ±0.003

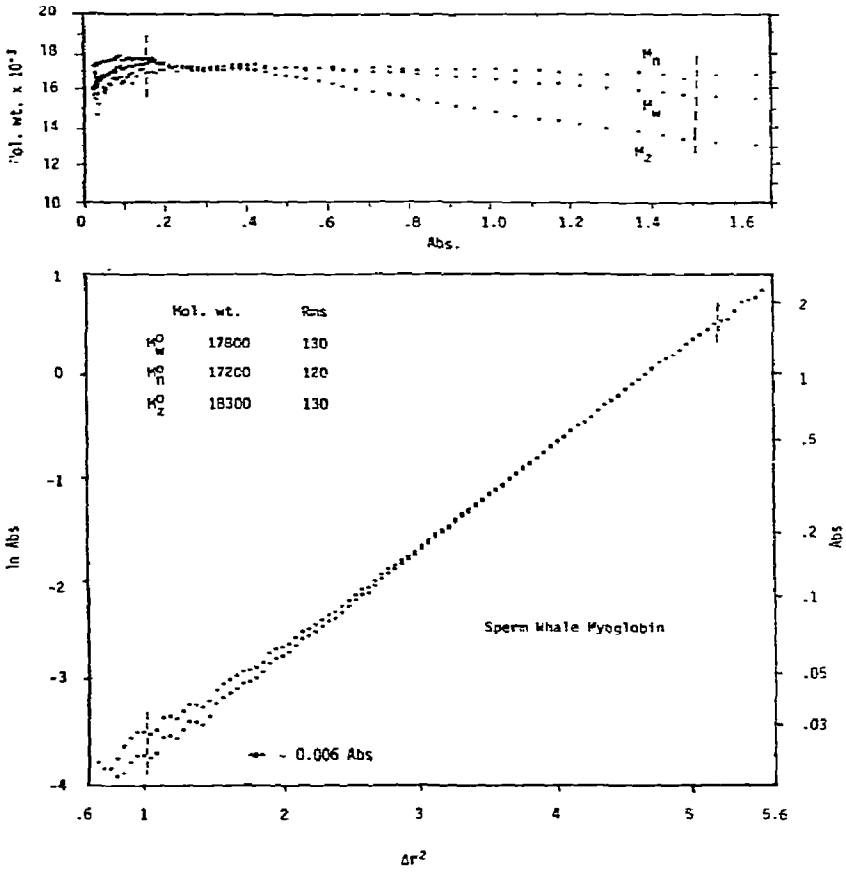

Fig. 8. Sedimentation equilibrium of sperm whale myoglobin. Two 4° single-sector cells filled to a 4 mm height, one with protein and one with solvent (0.05 M sodium phosphate, pH 7.0) were sedimented overnight at 32 000 rpm at 15°C. 330 scans were accumulated with SIT gain of about 100 and a 3.2° gate. The light at 435 nm was attenuated with a 1.9 optical density neutral density filter.

units each for the solvent and solution intensity patterns.) A sliding least-squares quadratic fit of groups of 15 points (with no "smoothing") gave the value for M_n, M_w, and M_z plotted versus the absorbance in fig. 8. The values extrapolated to zero absorbance are in satisfactory agreement with the value of 17 199 based upon amino acid analysis [11].

Thus it appears that, for this experiment, the partial defocusing of the intensifier stage did not affect the absorbance measurements. In other experiments a downward curvature in the ln absorbance versus r^2 plots in the region of the cell bottom may have arisen from defocusing.

7.3. Current work

Even though our mark detector system is satisfactory and detection of a mark on the side of the rotor has greater inherent accuracy than detection of a similar mark on the rotor collar, the latter approach leads to simpler mechanical construction. During our tests in the two other laboratories we had an opportunity to examine the use of Beckman rotor collars. Dr. Marc S. Lewis has used the Beckman collar with his multiplexer circuit for pulsing a laser. A signal was picked up early in his circuit and then passed through an interface to our controller system. The phase-locked loop circuit worked well, but we did not have the

opportunity to examine pulse shapes with a high frequency oscilloscope.

We plan to construct a collar system, but with a single stripe. With the smaller clearance available at the collar, it should be possible to use a photodiode lamp and the same photodiode detector, with its nonosecond rise time, that we are now using. If this combination has the capability of also resolving 0.1°, it then will be possible to install the entire OMA scanner system on a different ultracentrifuge in several hours.

We still have not determined the optimum gate width for pulsing the SIT, not have we evaluated the use of double-sector cells. We have performed a preliminary examination of SIT images with an improved power supply having no ripple and slightly sharper pulse edges, but still with rise and fall times of about 0.8 μs. With a rotor spinning at 44 000 rpm it was possible to narrow the gate angle and observe the actual high voltage pulse shape. The same light flux through the cell was maintained by removing neutral density filters. As the flat part of this pulse was narrowed, thereby enhancing the contribution of the defocused image, the sharpness of the reference edges diminished and the reference holes shifted away from the center of the pattern. When the pulse was narrowed to the extent that the flat region just disappeared, the pattern was reduced to a "hill" in the center with no reference holes.

By accumulation of an image for 3.0° pulses and then another image for the same number of scans but with narrower pulses having no flat region (0.4°), it was possible to estimate the contribution of the defocused portion of the pulse. The defocused portion represented about 8% of the total intensity in the center of the pattern, decreasing to essentially zero at the edges.

We need to perform more sedimentation equilibrium experiments and investiagte the effect of gate width on the ln absorbance versus r^2 plots. We plan to obtain a pulsed power supply with negligible rise and fall times (100 ns or less) and examine the quality of images obtained with narrow gates moved across the cell opening.

Most of our work with the SIT has been performed with light obtained from an H85C3 medium pressure mercury arc lamp with a 2.5 mm square aperture and interference filters to obtain the desired wavelength – 365, 435, or 546 nm. The light intensity is so high that neutral density filters must be added to eliminate from 90 to 99% of the light, even with the SIT operated at a gain of only 100 times.

In Dr. Howard K. Schachman's laboratory we were able to test the use of the standard Beckman DU monochrometer with the Hg–Xe lamp. With this source of light there is again excessive light at the visible Hg lines. (In fact, a Xe lamp should provide sufficient light at any visible wavelength.) However, the fiber-optics faceplate of the SIT absorbs all of the light for wavelengths below 350 nm. The manufacturers of the OMA have provided a fluorescent, transparent film which converts radiation below this wavelength, *but* with an efficiency of only 1–2% because of the wide angle of emission from the film and the narrow acceptance angle of the individual fibers in the SIT faceplate. There was still sufficient light at wavelengths corresponding to Hg lines down to 245 nm to see a full-scale image in real time. For light between 215–230 nm, only a small image was seen even after accumulation of many scans.

It must be emphasized that the low efficiency of the wavelength converter when used for UV light enhances the contribution of stray visible light 50 to 100 times.

We are currently constructing a monochrometer system from other components that should provide more light in the UV region.

8. Comparison of photomultiplier and OMA scanners

It is evident that with neither type of scanner has there been achieved the maximum accuracy possible. Further improvement in the accuracy of photomultiplier scanners will be achieved when there is general usage of the integrated pulse instead of the height. The phase-locked loop method for selection of gates might be the best approach for this purpose.

The principal advantage of the photomultiplier scanner is that there are already in existence many commercial installations with recorder outputs of absorbance profiles. A limited number of investigators have adapted the commercial scanner for minicomputer operation. From papers presented at this conference, it appears that improved accuracy lags improved data processing. The main disadvantage of the

photomultiplier scanner is that, apparently, the detector itself has reached the limit of performance.

The television scanner has become possible in recent years because of the commercial and military need for a low-level light image device. The use of the OMA as the detector for a television scanner has the obvious advantage of its being used for a variety of other applications requiring detection of light at low levels. The manufacturer of the OMA has a more aggressive, ongoing research and development program compared to the manufacturer of the commercial photomultiplier scanner. A new detector head (Model 1205I) has recently been introduced, which has ten times the gain of the SIT. It employs an "intensified SIT" camera tube, which has another intensifier stage that can be gated. It is likely that improved camera tubes will become available in the future. The incorporation of different tubes into the OMA system would require, at most, a new head assembly, relatively small changes in circuitry, and perhaps an additional power supply.

The removal of the OMA detector head is a simple matter, and its realignment requires only a few seconds. (Several times we have used the OMA with an optical system for study of the sedimentation of living cells at unit gravity.) The ability to see the whole image in real time considerably simplifies the alignment of the entire optical system.

As with the photomultiplier system, one can also use the television scanner to detect rotor precession, but only if the period is several times longer than the 32.8 ms scan time. The effect of rotor precession on absorbance patterns is different for the two scanners. With the scanned photomultiplier slit, precession appears as a sinusoidal variation of the absorbance trace [12]. Precession for the television scanner produces an effect equivalent to averaging the intensity profile through a slit. The latter alteration of an absorbance pattern is less serious.

The photomultiplier scanner has the potential of translational warpage arising from uneveness in the screw pitch and also from random "flutter" during the scanning process. We know that the SIT has a slight radial warpage arising from pincushion distortion in the intensifier stage. Careful examination of channel positions on the monitor screen revealed that the only observable shift was in the entire image, which was attributable to rotor precession. Thus there is no "flutter" in individual channel positions relative to others. We are currently evaluating the effect of channel distortion using a quartz ruled disc with 0.5 mm line spacing.

Acknowledgement

We greatly appreciate the support of the National Heart and Lung Institute for this work (grant number HL14938). The early developmental work with the SIT would not have been possible without the suggestions and help of Dr. M.R. Zatzick. We are thankful to Drs. Howard K. Schachman and Marc S. Lewis for knowledge gained from setting up and using the OMA in their laboratories.

References

[1] Theodor Svedberg and H. Rinde, J. Am. Chem. Soc. 46 (1924) 2577.
[2] S. Hanlon, K. Lamers, G. Lauterbach, R. Johnson and H.K. Schachman, Arch. Biochem. Biophys. 99 (1962) 157.
[3] K. Lamers, F. Putney, I.Z. Steinberg and H.K. Schachman, Arch. Biochem. Biophys. 103 (1963) 379.
[4] S.P. Spragg, S. Travers and T. Saxton, Anal. Biochem. 12 (1965) 259.
[5] P.H. Lloyd and M.P. Esnouf, Anal. Biochem. 60 (1974) 25.
[6] E.G. Richards and D. Rockholt, Arch. Biochem. Biophys. 158 (1973) 864.
[7] H.K. Schachman and S.J. Edelstein, Biochemistry 5 (1966) 2681.
[8] C.H. Paul and D.A. Yphantis, Anal. Biochem. 48 (1972) 605.
[9] R. Cohen, J. Cluzel, H. Cohen, P. Male, M. Moignier and C. Soulié, Biophys. Chem. 5 (1976) 77.
[10] M.S. Springer and H.K. Schachman, Biochemistry 13 (1974) 3726.
[11] A.B. Edmunson, Nature (London) 205 (1965) 883.
[12] D.C. Teller, in: Methods in Enzymology, Vol. 27, eds. C.H.W. Hirs and S.W. Timashef (Academic Press, New York, 1973) p. 359.